ENGINEERING TRANSACTIONS • *Engng. Trans.* • **51**, 1, 3–24, 2003
Polish Academy of Sciences • Institute of Fundamental Technological Research
10.24423/engtrans.498.2003

THE INVESTIGATION OF THE INFLUENCE OF A LOCAL ELASTIC NONLINEARITY ON VIBRATIONS OF PLANE TRUSS MEMBERS

A. Pielorz

Institute of Fundamental Technological Research,
Polish Academy of Sciences
21 Świętokrzyska Str., 00-049 Warsaw, Poland

The paper concerns theoretical investigations of plane trusses subject to longitudinal deformations, using nonlinear discrete-continuous models. An external excitation is applied to a rigid body located in a truss joint. In this joint a visco-elastic discrete element with a spring having a nonlinear symmetric stiffness is also located. It is assumed that the spring characteristic is of a soft type. Four nonlinear functions describing this characteristic are proposed. In the considerations the wave method is applied similarly to the case of a hard characteristic in [1]. The numerical analysis focus on the investigation of the effect of the local nonlinearity with a soft characteristic for two examples of plane trusses.

Key words: nonlinear dynamics, discrete-continuous models, plane trusses

1. Introduction

The considerations concentrate on the analysis of dynamics of plane trusses with a local nonlinearity. In the discussion, discrete-continuous models consisting of members and of rigid bodies are used. This concerns trusses with joints idealised as hinges without friction. In such cases, truss members are subject only to longitudinal deformations, [2]. The deformation of the truss is assumed to be sufficiently small, so that the change of the geometry of the truss can be neglected. The mass of the drive system mating with the truss is also taken into account as a part of the mass of the rigid body. Rigid bodies in the models are concentrated masses being in translatory motion. The external force can be described by an arbitrary function, periodic or nonperiodic. In the discrete-continuous model, additional discrete elements can be introduced. These elements consist of a spring and a damper and represent the influence of adjoining truss members. The spring may have a linear as well as a nonlinear characteristic.

Linear discrete-continuous models of plane trusses are discussed in [3]. Nonlinear discrete-continuous models with the local nonlinearity having the characteristic of a hard type are studied in [1]. The aim of the present paper is to consider similar models as in [1], however the local nonlinearity has the characteristic of a soft type. The inclusion of such types of nonlinearities is justified by many engineering solutions for plane trusses, [2, 4]. The force in the nonlinear spring is described by means of four nonlinear functions: 1) the polynomial of the third degree, 2) the sinusoidal function, 3) the hyperbolic tangent function, and 4) the exponential function. Such types of functions are justified by numerous experimental studies, [5]. The polynomial function can be used in the case of a spring having the soft as well as hard characteristic, while the remaining ones – only for soft characteristics. The introduction of four different functions not only expands the discussion on the local nonlinearities but also enables to avoid such effects as the escape from potential wells which may appear in numerical solutions for nonlinear models. Some examples of this escape are shown in [6] for discrete models.

In the discussion, the wave method resulting from the method of characteristics, is applied, similarly as in [1, 3]. In numerical calculations, the influence of the local nonlinearity on displacements for two models of plane trusses is investigated.

It should be pointed out that trusses have always been investigated intensively. Particularly, their static investigations have a rich and long-lasting tradition, [2, 4, 7]. Not many papers deal with dynamic investigations of truss members, e.g. [8–10]. They concern mainly impact problems in trusses with massless joints, taking into account elastic as well as plastic materials of truss members. The obtained results are limited to very short time intervals of the order of microseconds, while in the present paper the nonlinear models of plane trusses with long-lasting loading are studied.

2. Assumptions, nonlinear forces

Consider the nonlinear discrete-continuous model of a plane truss consisting of an arbitrary number of truss members connected by rigid bodies, and of viscoelastic discrete elements, as shown in Fig. 1. The cross-sections of members are constant. Members are subject only to longitudinal deformations. It is assumed that at the time instant $t = 0$, displacements and velocities of cross-sections of truss members are equal to zero. A real damping of truss members is represented by an equivalent damping applied in selected cross-sections of the members in the model. The i-th member is characterised by the Young modulus E, density ρ, the length l_i and the cross-section area A. The j-th rigid body having the concentrated mass m_j undergoes the translatory motion.

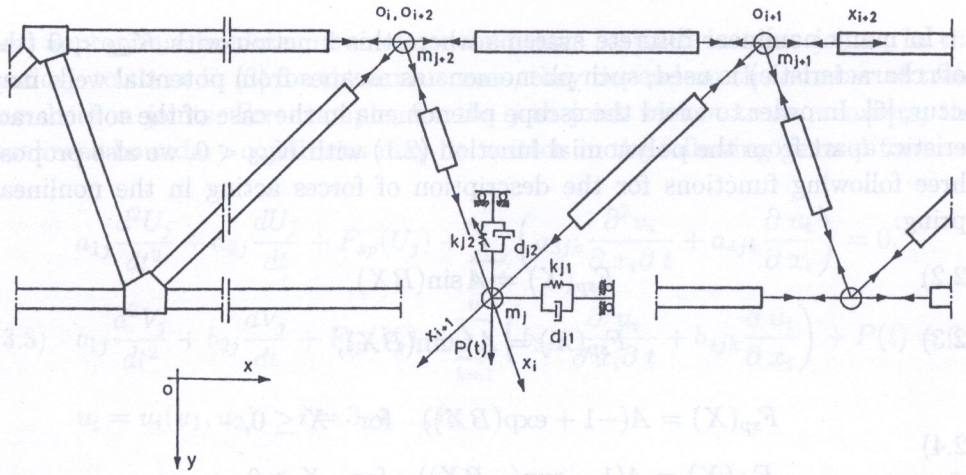

FIG. 1. Nonlinear model of a plane truss.

In the description of the nonlinear discrete-continuous model, a fixed reference system $0xy$, and one-dimensional coordinate systems $0_i x_i$ assigned to individual i-th truss members are used. The origin of $0_i x_i$ system coincides with the location of one of the ends of the i-th member in the undisturbed state at $t = 0$. In this connection, the displacement of the cross-section x_i in the i-th truss member is described by the function $u_i(x_i, t)$ depending on the location of the considered cross-section and on time, whereas the time functions U_j, V_j are the components of the displacements of the j-th rigid body in the x-axis and y-axis directions, respectively.

In the considered discrete-continuous model, a single local nonlinearity by means of a nonlinear discrete spring is taken into account. This element can be located in any cross-section where a rigid body is loaded by an external force $P(t)$ and is fixed by elements which have a nonlinear characteristic.

The moment of a nonlinear spring can be generally described by an arbitrary nonlinear function, [5]. In the discussion of the dynamics of nonlinear discrete systems, a polynomial of the third degree is exploited most widely for the description of the considered nonlinearities, [6, 11]. In the present paper it is used in the case of the discrete-continuous systems. Analogously to nonlinearities in discrete systems, the force acting in the nonlinear spring with a symmetric characteristic could be described by the following function

$$F_{sp}(X) = K_{w1}X + K_{w3}X^3, \tag{2.1}$$

where X is an appropriate displacement and K_{w1} and K_{w3} represent linear and nonlinear terms in (2.1), respectively. The polynomial (2.1) includes the soft characteristic for $K_{w3} < 0$, the linear case for $K_{w3} = 0$ and the hard characteristic for $K_{w3} > 0$.

In many nonlinear discrete systems where this function with $K_{w3} < 0$ (the soft characteristic) is used, such phenomena as escapes from potential wells may occur, [6]. In order to avoid the escape phenomena in the case of the soft characteristic, apart from the polynomial function (2.1) with $K_{w3} < 0$, we also propose three following functions for the description of forces acting in the nonlinear spring:

$$F_{sp}(X) = A\sin(BX), \tag{2.2}$$

$$F_{sp}(X) = A\tanh(BX), \tag{2.3}$$

$$\begin{aligned} F_{sp}(X) &= A(-1+\exp(BX)) \quad \text{for} \quad X \leq 0, \\ F_{sp}(X) &= A(1-\exp(-BX)) \quad \text{for} \quad X \geq 0, \end{aligned} \tag{2.4}$$

where the constants A and B are selected in such a way that the expansions in series of functions (2.2) – (2.4) give the same linear case and that the polynomial function (2.1) is the approximation of the sinusoidal function (2.2). Then the function (2.1) and the functions (2.2) – (2.4) have maximum values close to each other, and

$$AB = K_{w1}, \quad AB^3 = -6K_{w3}. \tag{2.5}$$

Below, especially when describing the numerical results, the nonlinear functions (2.1) – (2.4) will be called the functions (1) – (4), for simplicity.

3. Governing equations

Under the above assumptions, the equation of motion for the i-th truss member is the classical wave equation

$$\frac{\partial^2 u_i(x_i,t)}{\partial t^2} - a^2\frac{\partial^2 u_i(x_i,t)}{\partial x_i^2} = 0 \quad \text{for} \quad 0 < x_i < l_i \tag{3.1}$$

where $a^2 = E/\rho$.

Equations with the damping continuously distributed should better describe the motion of truss members. However, no effective methods have been developed as far for solving appropriate equations of motion in the case of discrete-continuous models. For this reason, the damping is described by an equivalent internal and external damping taken into account in the boundary conditions.

In order to find solutions for specific nonlinear cases, we must add to equations (3.1) the following initial conditions:

$$u_i(x_i,0) = \frac{\partial u_i}{\partial t}(x_i,0) = 0 \tag{3.2}$$

and appropriate nonlinear boundary conditions satisfied in truss joints. In the analogy to those in [3] for the linear cases, they depend on the number of truss members in joints. For example, for the j-th joint with n truss members, the nonlinear boundary conditions may be written in the following general form:

$$
\begin{aligned}
&a_{1j}\frac{d^2U_j}{dt^2}+a_{2j}\frac{dU_j}{dt}+F_{sp}(U_j)+\sum_{k=1}^{n}\left(a_{3jk}\frac{\partial^2 u_i}{\partial\, x_i \partial\, t}+a_{4jk}\frac{\partial\, u_i}{\partial\, x_i}\right)=0,\\
&b_{1j}\frac{d^2V_j}{dt^2}+b_{2j}\frac{dV_j}{dt}+F_{sp}(V_j)+\sum_{k=1}^{n}\left(b_{3jk}\frac{\partial^2 u_i}{\partial\, x_i \partial\, t}+b_{4jk}\frac{\partial\, u_i}{\partial\, x_i}\right)+P(t)=0, \qquad (3.3)\\
&u_i=u_i(u_1,u_2), \quad i=3,4,...,n,
\end{aligned}
$$

where a_{1j} and b_{1j} are determined by the mass m_j, a_{2j} and b_{2j} represent coefficients of external damping, a_{3jk} and b_{3jk} represent the internal damping of the Voigt type in successive truss members, a_{4jk}, b_{4jk} are determined by material constants, and the functions $F_{sp}(U_j)$ and $F_{sp}(V_j)$ represent local nonlinearities in the model. In [3] $F_{sp}(U_j)$ and $F_{sp}(V_j)$ are linear functions.

The components U_j, V_j of the displacement of the j-th joint in the plane truss may be described by the displacements of an arbitrary pair of truss members in the joint. The conditions (3.3) are written for the case when they are determined by appropriate displacements u_1, u_2 of the first two truss members in the j-th joint. This assumption does not reduce the generality of the considerations. In analogy to static displacements, it is shown in [3] that if z_i corresponds to the displacement u_i of the end of the i-th truss member in the j-th joint, then the functions U_j, V_j and relations needed in boundary conditions (3.3) have the form

$$
\begin{aligned}
&U_j=(z_k\cos\alpha_i-z_i\cos\alpha_k)\sin^{-1}(\alpha_k-\alpha_i),\\
&V_j=(z_i\sin\alpha_k-z_k\sin\alpha_i)\sin^{-1}(\alpha_k-\alpha_i), \qquad (3.4)\\
&z_i\sin(\alpha_2-\alpha_1)=z_2\sin(\alpha_i-\alpha_1)-z_1\sin(\alpha_i-\alpha_2), \quad i=2,3,...,n
\end{aligned}
$$

where $i<k$ and α_i is the angle between the i-th truss member and the y-axis, $i=1,2,...,n$, [3]. The relations (3.4) are derived under the assumptions that the angles α_i remain constant during the motion of the truss and that z_i are orthogonal projections of the displacements of the ends of the i-th truss members. The truss members undergo small deformations and small displacements, so the above assumptions are justifiable, [2, 3].

Taking into account initial conditions (3.2), one could seek for the solution of equations (3.1) in the form

$$
u_i(x_i,t)=f_i(a(t-t_{fi})-x_i+x_{fi})+g_i(a(t-t_{gi})+x_i-x_{gi}), \qquad (3.5)
$$

where the functions f_i, g_i represent disturbances caused by the external force $P(t)$ in the i-th truss member in a direction consistent and opposite to the direction of the x-axis, respectively. The constants $t_{fi}, t_{gi}, x_{fi}, x_{gi}$ in the arguments of these functions denote the time instant and the location of the end of the i-th member in which the first disturbance is observed in this member. These constants may be equal or differ from each other. The functions f_i, g_i are continuous functions of a single variable, and for negative arguments they are identically equal to zero. Their forms are determined by boundary conditions for particular problems. Upon substituting the solution (3.5) into appropriate nonlinear boundary conditions, nonlinear ordinary differential equations with a retarded argument are obtained for unknown functions f_i, g_i.

The approach described above one can use for the consideration of complex nonlinear discrete-continuous models similar to that shown in Fig. 1. However, in the present paper, detailed investigations are made for two specific segments of the plane truss. It should be pointed out that nonlinear discrete-continuous models of trusses have not been known in the available technical literature. Moreover, simple nonlinear models lead to solving a smaller number of nonlinear equations, and in spite of simplification they can give useful information on dynamic behaviour of nonlinear models for plane trusses.

4. Specific cases of nonlinear models of a plane truss

Real trusses usually consist of repeated segments. Below, we discuss two nonlinear models of segments where the influence of adjoining truss portions are taken into account by means of discrete elements consisting of a spring and a damper. It is assumed that one of springs has a nonlinear stiffness of a soft type. The studied nonlinear models differ from linear models of segments considered in [3] by a nonlinear spring located in the joint where an external loading is applied, and differ from that discussed in [1] since now the soft characteristic is described by means of four nonlinear functions (2.1) – (2.4).

The nonlinear model of a truss segment is shown in Fig. 2. It consists of 3 truss members having the lengths l_1, l_2, l_3. This model may be treated as a part of the model of the plane truss shown in Fig. 1. In the description of the model we use a fixed reference system $0xy$ and one-dimensional coordinate systems $0_i x_i$ assigned to the members, $i = 1, 2, 3$. The truss members (1), (2) and the y-axis make angles α, β, respectively.

In the model, a rigid body m_1 is located in the joint with coordinates $x = 0$, $y = l_1 \cos\alpha$ ($x_1 = l_1$, $x_2 = l_2$). This rigid body represents both the mass of a drive system mating with the truss and the mass of the element connecting truss members (1), (2). It is loaded by an external force $P(t)$ acting in the y-axis direction. The force and the member reaction cause the rigid

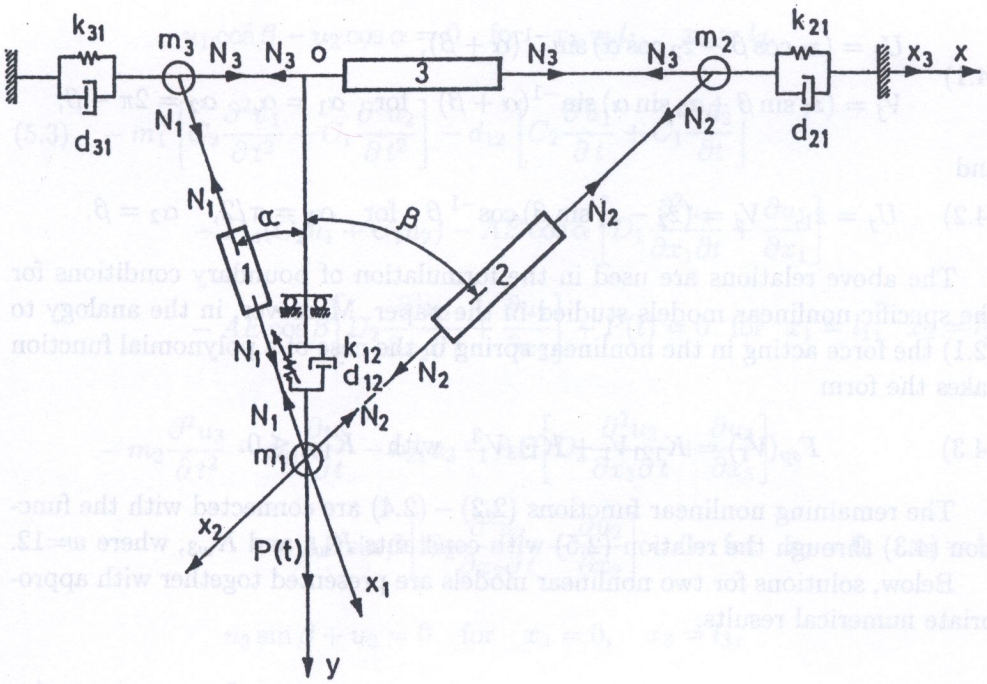

FIG. 2. Nonlinear discrete-continuous model of the segment of a plane truss.

body m_1 to displace in the plane xy. For the simplicity, it is assumed that the displacement of this rigid body in the x-axis direction is equal to zero ($U_1 \equiv 0,\ V_1 \neq 0$). The rigid body m_1 is connected with a nonlinear discrete element in y-axis, with the nonlinear stiffness of the spring and with the damping coefficient d_{12}. The rigid body m_2 is located in the joint of coordinates $x = l_2 \sin\beta,\ y = 0$ ($x_2 = 0,\ x_3 = l_3$). It displaces only in the x-axis direction ($U_2 \neq 0,\ V_2 \equiv 0$). A discrete element with coefficients k_{21}, d_{21} representing the effect of adjoining truss members, is attached to this body. It is assumed that in the joint $x = -l_1 \sin\alpha,\ y = 0$ ($x_1 = 0,\ x_3 = 0$), the rigid body m_3 displacing only along x-axis direction ($U_3 \neq 0,\ V_3 \equiv 0$) is located. A discrete element with coefficients k_{31} and d_{31}, representing the influence of adjoining truss members, is attached to the rigid body m_3.

As a second nonlinear model of truss segments we consider a model described above in the case when the mass m_3 is equal to zero and the ends of members (1) and (3) in the joint $x = -l_1 \sin\alpha,\ y = 0$ are fixed. The suitable figure of this model results from Fig. 2 and for this reason it is not shown in the present paper, see [3].

The joints in the models considered in the paper bond two truss members. In such cases the relations (3.4), valid for n-member joints, reduce to

$$
\begin{aligned}
U_j &= (z_1 \cos\beta - z_2 \cos\alpha)\sin^{-1}(\alpha+\beta), \\
V_j &= (z_1 \sin\beta + z_2 \sin\alpha)\sin^{-1}(\alpha+\beta) \quad \text{for} \quad \alpha_1 = \alpha, \quad \alpha_2 = 2\pi - \beta,
\end{aligned} \tag{4.1}
$$

and

$$
U_j = z_1, \quad V_j = (z_2 - z_1 \sin\beta)\cos^{-1}\beta \quad \text{for} \quad \alpha_1 = \pi/2, \quad \alpha_2 = \beta. \tag{4.2}
$$

The above relations are used in the formulation of boundary conditions for the specific nonlinear models studied in the paper. Moreover, in the analogy to (2.1) the force acting in the nonlinear spring in the case of a polynomial function takes the form

$$
F_{sp}(V_1) = K_{121}V_1 + K_{123}V_1^3 \quad \text{with} \quad K_{123} \leq 0. \tag{4.3}
$$

The remaining nonlinear functions (2.2) – (2.4) are connected with the function (4.3) through the relation (2.5) with constants K_{w1} and K_{w3}, where w=12.

Below, solutions for two nonlinear models are presented together with appropriate numerical results.

5. Solution of the nonlinear model I.

The first nonlinear model discussed here is shown in Fig. 2. If one takes into account Eqs. (3.1) – (3.5) and (4.1) – (4.3), the determination of displacements for truss members (1) – (3) of the Model I is reduced to solving the equations

$$
\frac{\partial^2 u_i(x_i,t)}{\partial t^2} - a^2 \frac{\partial^2 u_i(x_i,t)}{\partial x_i^2} = 0 \quad \text{for} \quad i = 1,2,3 \tag{5.1}
$$

with the initial conditions

$$
u_i(x_i,0) = \frac{\partial u_i}{\partial t}(x_i,0) = 0 \quad \text{for} \quad i = 1,2,3 \tag{5.2}
$$

and the following nonlinear boundary conditions

$$
\begin{aligned}
-m_3\frac{\partial^2 u_3}{\partial t^2} - d_{31}\frac{\partial u_3}{\partial t} - k_{31}u_3 + AE\left[D_3\frac{\partial^2 u_3}{\partial x_3 \partial t} + \frac{\partial u_3}{\partial x_3}\right] \\
+ AE\sin\alpha\left[D_1\frac{\partial^2 u_1}{\partial x_1 \partial t} + \frac{\partial u_1}{\partial x_1}\right] = 0 \quad \text{for} \quad x_1 = x_3 = 0,
\end{aligned}
$$

$$
-u_3\sin\beta + u_1 = 0 \quad \text{for} \quad x_1 = x_3 = 0,
$$

$$u_1 \cos\beta - u_2 \cos\alpha = 0 \quad \text{for} \quad x_1 = l_1, \quad x_2 = l_2,$$

$$(5.3)\quad - m_1 \left[C_2 \frac{\partial^2 u_1}{\partial t^2} + C_1 \frac{\partial^2 u_2}{\partial t^2} \right] - d_{12} \left[C_2 \frac{\partial u_1}{\partial t} + C_1 \frac{\partial u_2}{\partial t} \right]$$

$$- F_{sp}(C_2 u_1 + C_1 u_2) - AE \cos\alpha \left[D_1 \frac{\partial^2 u_1}{\partial x_1 \partial t} + \frac{\partial u_1}{\partial x_1} \right]$$

$$- AE \cos\beta \left[D_2 \frac{\partial^2 u_2}{\partial x_2 \partial t} + \frac{\partial u_2}{\partial x_2} \right] + P(t) = 0 \quad \text{for} \quad x_1 = l_1, \quad x_2 = l_2,$$

$$- m_2 \frac{\partial^2 u_3}{\partial t^2} - d_{21} \frac{\partial u_3}{\partial t} - k_{21} u_3 - AE \left[D_3 \frac{\partial^2 u_3}{\partial x_3 \partial t} + \frac{\partial u_3}{\partial x_3} \right]$$

$$- AE \sin\beta \left[D_2 \frac{\partial^2 u_2}{\partial x_2 \partial t} + \frac{\partial u_2}{\partial x_2} \right] = 0 \quad \text{for} \quad x_2 = 0, \quad x_3 = l_3,$$

$$u_3 \sin\beta + u_2 = 0 \quad \text{for} \quad x_2 = 0, \quad x_3 = l_3,$$

where

$$(5.4)\quad C_1 = \frac{\sin\alpha}{\sin\xi}, \quad C_2 = \frac{\sin\beta}{\sin\xi}, \quad \xi = \alpha + \beta.$$

Upon the introduction of nondimensional quantities

$$(5.5)\quad \begin{aligned} &\bar{x}_i = x_i / l_0, \quad \bar{t} = at/l_0, \quad \bar{u}_i = u_i/u_0, \quad \bar{d}_{ij} = d_{ij} l_0/(am_0), \\ &\bar{D}_i = aD_i/l_0, \quad R_i = m_i/m_0, \quad K_0 = A\rho l_0/m_0, \quad \bar{P} = P l_0^2/(m_0 u_0 a^2), \\ &\bar{k}_{ij} = k_{ij} l_0^2/(m_0 a^2), \quad \bar{l}_i = l_i/l_0, \quad \bar{K}_{121} = K_{121} l_0^2/(m_0 a^2), \\ &\bar{K}_{123} = K_{123}\, u_0^2 l_0^2/(m_0 a^2), \quad \bar{F}_{sp} = F_{sp} l_0^2/(m_0 u_0 a^2) \end{aligned}$$

relations (5.1) – (5.3) take the form

$$(5.6)\quad \frac{\partial^2 u_i(x_i,t)}{\partial t^2} - \frac{\partial^2 u_i(x_i,t)}{\partial x_i^2} = 0 \quad \text{for} \quad i = 1,2,3,$$

$$(5.7)\quad u_i(x_i,0) = \frac{\partial u_i}{\partial t}(x_i,0) = 0 \quad \text{for} \quad i = 1,2,3,$$

$$- R_3 \frac{\partial^2 u_3}{\partial t^2} - d_{31} \frac{\partial u_3}{\partial t} - k_{31} u_3 + K_0 \left[D_3 \frac{\partial^2 u_3}{\partial x_3 \partial t} + \frac{\partial u_3}{\partial x_3} \right]$$

$$+ K_0 \sin\alpha \left[D_1 \frac{\partial^2 u_1}{\partial x_1 \partial t} + \frac{\partial u_1}{\partial x_1} \right] = 0 \quad \text{for} \quad x_1 = x_3 = 0,$$

$$-u_3 \sin\beta + u_1 = 0 \quad \text{for} \quad x_1 = x_3 = 0,$$

$$u_1 \cos\beta - u_2 \cos\alpha = 0 \quad \text{for} \quad x_1 = l_1, \quad x_2 = l_2,$$

$$\begin{aligned}(5.8)\quad & -R_1\left[C_2\frac{\partial^2 u_1}{\partial t^2} + C_1\frac{\partial^2 u_2}{\partial t^2}\right] - d_{12}\left[C_2\frac{\partial u_1}{\partial t} + C_1\frac{\partial u_2}{\partial t}\right] \\ & - F_{sp}(C_2u_1 + C_1u_2) - K_0\cos\alpha\left[D_1\frac{\partial^2 u_1}{\partial x_1 \partial t} + \frac{\partial u_1}{\partial x_1}\right] \\ & - K_0\cos\beta\left[D_2\frac{\partial^2 u_2}{\partial x_2 \partial t} + \frac{\partial u_2}{\partial x_2}\right] + P(t) = 0 \quad \text{for} \quad x_1 = l_1, \quad x_2 = l_2,\end{aligned}$$

$$\begin{aligned}& -R_2\frac{\partial^2 u_3}{\partial t^2} - d_{21}\frac{\partial u_3}{\partial t} - k_{21}u_3 - K_0\left[D_3\frac{\partial^2 u_3}{\partial x_3 \partial t} + \frac{\partial u_3}{\partial x_3}\right] \\ & - K_0\sin\beta\left[D_2\frac{\partial^2 u_2}{\partial x_2 \partial t} + \frac{\partial u_2}{\partial x_2}\right] = 0 \quad \text{for} \quad x_2 = 0, \quad x_3 = l_3,\end{aligned}$$

$$u_3 \sin\beta + u_2 = 0 \quad \text{for} \quad x_2 = 0, \quad x_3 = l_3,$$

where bars are omitted for convenience, and l_0, u_0, m_0 are fixed values of the length, displacement and mass, respectively.

According to Eq. (3.5), the solutions of equations (5.6), taking into account (5.7), are sought in the form

$$\begin{aligned}(5.9)\quad & u_1(x_1,t) = f_1(t - x_1 + l_1) + g_1(t + x_1 - l_1), \\ & u_2(x_2,t) = f_2(t - x_2 + l_2) + g_2(t + x_2 - l_2), \\ & u_3(x_3,t) = f_3(t - l_1 - x_3) + g_3(t - l_2 + x_3 - l_3).\end{aligned}$$

In the considered model the disturbances caused by the external force $P(t)$ arrive to the member (3) through the member (1) as well as through the member (2). Thus, according to (3.5) it is taken into account in (5.9), that $t_{f3} = l_1$ and $x_{f3} = 0$ while $t_{g3} = l_2$ and $x_{g3} = l_3$.

Substituting (5.9) into the nonlinear boundary conditions (5.8), and denoting the largest argument in each equality by z, one obtains the following equations

for 6 unknown functions $f_i, g_i, i = 1, 2, 3$:

$$f_1(z) = -g_1(z - 2l_1) + [f_3(z - 2l_1) + g_3(z - l_1 - l_2 - l_3)] \sin\beta,$$

$$f_2(z) = -g_2(z - 2l_2) - [f_3(z - l_1 - l_2 - l_3) + g_3(z - 2l_2)] \sin\beta,$$

$$r_1 g_1''(z) = P(z) + r_2 g_1'(z) + r_3 f_1''(z) + r_4 f_1'(z) + r_5 f_2''(z) + r_6 f_2'(z) - F_{sp}\left(\frac{f_1(z) + g_1(z)}{cos\alpha}\right),$$

$$g_2(z) = -f_2(z) + [f_1(z) + g_1(z)] \cos\beta / \cos\alpha, \tag{5.10}$$

$$r_7 g_3''(z) + r_8 g_3'(z) + r_9 g_3(z) = r_{10} f_3''(z - l_1 + l_2 - l_3) + r_{11} f_3'(z - l_1 + l_2 - l_3) + r_{12} f_3(z - l_1 + l_2 - l_3) + r_{13} g_2''(z) + r_{14} g_2'(z),$$

$$r_{15} f_3''(z) + r_{16} f_3'(z) + r_{17} f_3(z) = r_{18} g_3''(z + l_1 - l_2 - l_3) + r_{19} g_3'(z + l_1 - l_2 - l_3) + r_{20} g_3(z + l_1 - l_2 - l_3) + r_{21} g_1''(z) + r_{22} g_1'(z),$$

where

$$r_1 = R_1/\cos\alpha + K_0(D_1 \cos\alpha + D_2 \cos^2\beta/\cos\alpha),$$

$$r_2 = -d_{12}/\cos\alpha - K_0(\cos\alpha + \cos^2\beta/\cos\alpha),$$

$$r_3 = -R_1/\cos\alpha + K_0(D_1 \cos\alpha - D_2 \cos^2\beta/\cos\alpha),$$

$$r_4 = -d_{12}/\cos\alpha + K_0(\cos\alpha - \cos^2\beta/\cos\alpha),$$

$$r_5 = 2K_0 D_2 \cos\beta, \quad r_6 = 2K_0 \cos\beta,$$

$$r_7 = R_2 + K_0(D_3 + D_2 \sin^2\beta), \quad r_8 = d_{21} + K_0(1 + \sin^2\beta),$$

$$r_9 = k_{21}, \quad r_{10} = -R_2 + K_0(D_3 - D_2 \sin^2\beta), \tag{5.11}$$

$$r_{11} = -d_{21} + K_0(1 - \sin^2\beta), \quad r_{12} = -k_{21}, \quad r_{13} = -2K_0 D_2 \sin\beta,$$

$$r_{14} = -2K_0 \sin\beta, \quad r_{15} = R_3 + K_0(D_1 \sin\alpha \sin\beta + D_3),$$

$$r_{16} = d_{31} + K_0(\sin\alpha \sin\beta + 1), \quad r_{17} = k_{31},$$

$$r_{18} = -R_3 + K_0(D_3 - D_1 \sin\alpha \sin\beta),$$

$$r_{19} = -d_{31} + K_0(1 - \sin\alpha \sin\beta), \quad r_{20} = -k_{31},$$

$$r_{21} = 2K_0 D_1 \sin\alpha, \quad r_{22} = 2K_0 \sin\alpha.$$

Equations (5.10) consist of one nonlinear equation and linear equations. Linear equations are solved by means of the finite differences method, and the nonlinear equation for the function $g_1(z)$ by means of the Runge-Kutta method. Having obtained the functions f_i, g_i and their derivatives, one can determine displacements, strains and velocities in arbitrary member cross-sections at an arbitrary time instant, [1, 3, 12].

The external force $P(t)$ occurring in (5.10) can be described by an arbitrary time function. In the paper it is taken in the form

$$P(t) = P_0 \sin(pt) \tag{5.12}$$

where p is a nondimensional loading frequency.

In numerical calculations, the following values of dimensional quantities are assumed [3, 4]:

$$\begin{aligned} &l_0 = l_1 = l_2 = l_3 = 2\text{m}, \quad A = 2 \cdot 10^{-3}\text{m}^2, \quad \rho = 0.8 \cdot 10^4 \text{kg/m}^3, \\ &E = 2.1 \cdot 10^{11}\text{N/m}^2, \quad k_{ij} = K_{121} = 2.1 \cdot 10^8 \text{N/m}, \quad m_1 = 20\text{kg}, \\ &m_2 = m_3 = 3.2\text{kg}, \quad m_0 = 32\text{kg}, \quad a = 5000\text{m/s}, \\ &P_0 = 200\text{kN}, \quad u_0 = 10^{-3}\text{m}, \quad \alpha = \beta = \pi/6, \end{aligned} \tag{5.13}$$

whereas the values of nondimensional quantities according to (5.5) are

$$\begin{aligned} &R_1 = 0.625, \quad R_2 = R_3 = 0.1, \quad \bar{l}_i = 1.0, \\ &K_0 = 1.0, \quad \bar{P}_0 = 1.0, \quad \bar{k}_{ij} = \bar{K}_{121} = 1.05. \end{aligned} \tag{5.14}$$

The efficiency of the method applied in the paper is demonstrated in [3] for linear models of plane trusses giving the spatial diagrams of displacements in truss members and by investigating the influence of various parameters describing the considered models.

For this reason, in numerical calculations in the present paper we concentrate on the presentation of the influence of the local nonlinearity on displacements in selected member cross-sections.

For parameters given by (5.14) and damping coefficients equal to $d_{ij} = D_k = d_0 = 0.1$, displacements of the truss members (1), (2) are equal if $x_1 = x_2$, and displacements in the member (3) are antisymmetric with respect to the cross-section $x_3 = 0.5$.

From [1] it follows that the effect of the local nonlinearity can be investigated for an arbitrary cross-section of the considered truss members. In order to avoid too many diagrams, we concentrate on the study of this influence

on displacements V_1 of the rigid body m_1 located in the joint $x = 0$, $y = l_1 \cos\alpha$ ($x_1 = l_1$, $x_2 = l_2$). The displacement V_1 is expressed by $(4.1)_2$ with $z_1 = u_1(l_1, t)$, $z_2 = u_2(l_2, t)$, $\alpha_1 = \alpha$, $\alpha_2 = 2\pi - \beta$.

Nonlinear effects in the considered system are caused directly by the nonlinear force F_{sp} described by the functions (2.1) – (2.4). On the other hand, the nonlinear effects are also connected with the amplitude P_0 of the external loading and with the external and internal damping. In the performed numerical analysis, the damping coefficients are assumed to be constant equal to $d_{ij} = D_k = 0.1$.

The polynomial function (2.1) or rather (4.3) consists of the linear and nonlinear terms represented by coefficients K_{121} and K_{123}, respectively. In numerical calculations we fix the coefficient K_{121} while K_{123} can vary. If $K_{123} < 0$ then we propose to use also the functions (2.2) – (2.4) with coefficients A and B calculated from (2.5) for the given K_{121} and K_{123}. One can notice that the polynomial function (2.1) for $K_{123} < 0$ and the sinusoidal function (2.2) have their extremes and they can be useful for the values of their arguments between these extremes where the functions (2.1) and (2.2) are ascending functions. No limits of such a type are noted for the hyperbolic function (2.3) and the exponential function (2.4).

Numerical results given below are exemplary. In [1, 3] the amplitude-frequency curves are determined in various cross-sections of the considered systems. All diagrams in the present paper concern the cross-section where the nonlinear discrete element is taken into account. The discussion is focused on the influence of the parameters of this element having the characteristic of a soft type on displacements V_1, and on the nonlinear dynamic force F_{sp}.

In Fig. 3 amplitude-frequency curves for the displacement V_1 are plotted with $K_{123} = -0.05$, $P_0 = 0.5, 2.5$ and $p < 3.9$ using four functions (2.1) – (2.4) for the description of the nonlinear force F_{sp}. The diagrams corresponding to these functions are marked in figures by (1) – (4), for simplicity. The diagrams include two resonant regions. In the first resonant region for $P_0 = 0.5$ the functions (2.2) – (2.4) give similar results. Only using the function (2.1) we obtained the solution diverging to infinity in the neighbourhood of the resonance. Two extreme values of the frequency p are marked by spots. For $P_0 = 2.5$ the functions (2.3), (2.4) give practically the same results. Spots represent the extreme values of the frequency p where the solution with the function (2.1) starts to diverge to infinity, and the solution with the function (2.2) ceases to be a harmonic function. These marks defining the application ranges of the functions (2.1) and (2.2) occur in the first resonant region.

Amplitude-frequency curves for the nonlinear dynamic force are plotted in Fig. 4 for $K_{123} = -0.05$, $P_0 = 0.5$. From these diagrams it follows that the maximal values for dynamic forces occur for the sinusoidal function, and the smallest ones for the exponential function (2.4). Similarly to Fig. 3 for displacements, the

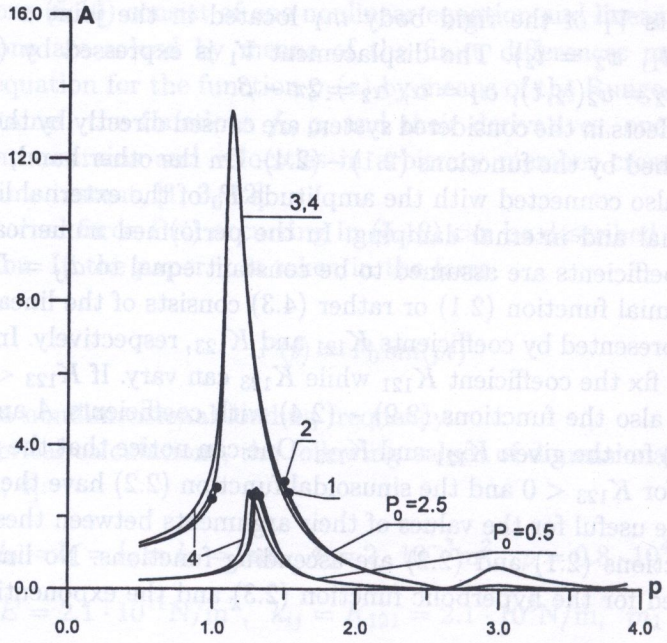

FIG. 3. Amplitude-frequency curves for displacements V_1 of the rigid body m_1 in the nonlinear Model I for $K_{123} = -0.05$, $P_0 = 0.5$, 2.5 with nonlinear functions (2.1) – (2.4).

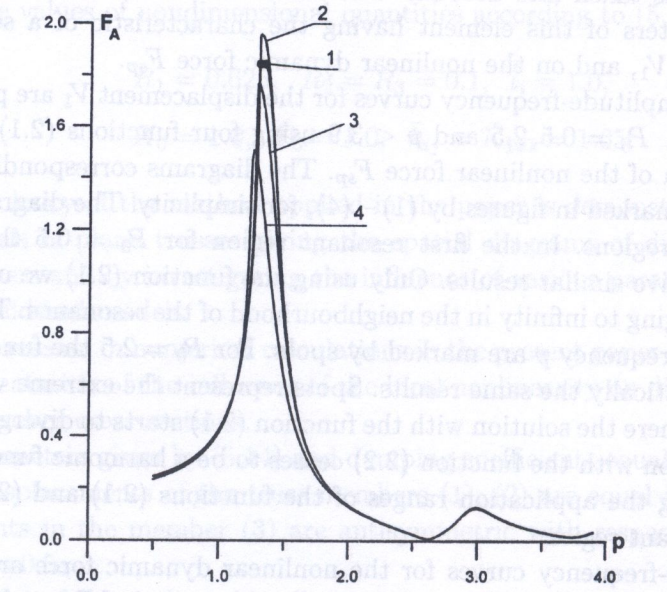

FIG. 4. Amplitude-frequency curves for dynamic force $F_{sp}(V_1)$ in the nonlinear Model I for $K_{123} = -0.05$, $P_0 = 0.5$ with nonlinear functions (2.1) – (2.4).

solution for the polynomial function has its interval for the frequency p where it diverges to infinity. This fact is marked by spots.

Amplitude-frequency curves for the dynamic force for $K_{123} = -0.05$, $P_0 = 2.5$ are plotted in Fig. 5. Similarly to Figs. 3 and 4, two resonant regions are taken into account. Now the effect of the local nonlinearity is stronger. The nonlinear forces (2.1) – (2.4) reach their maxima for assumed values of their coefficients. As this follows from the Fig. 5, the solutions with the functions (2.1) and (2.2) have the intervals where they are not of a harmonic type, and that is marked by spots. At the same intervals, the amplitudes for nonlinear force F_{sp} described by the functions (2.3) and (2.4) form the plateau.

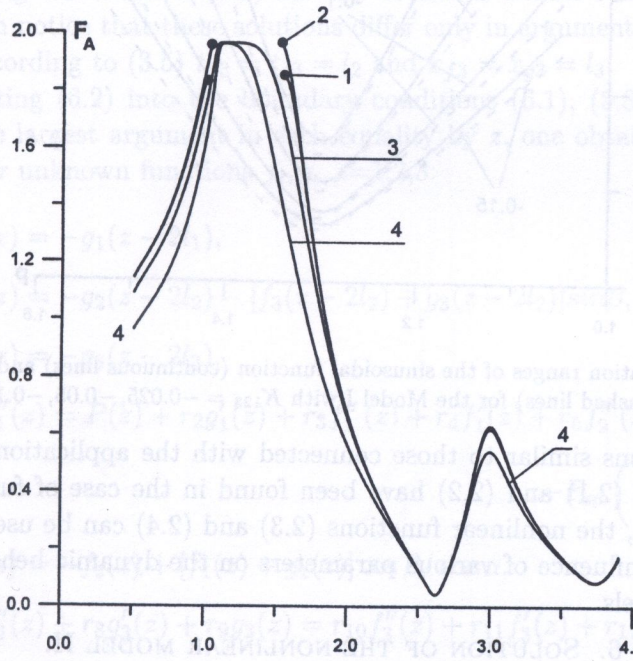

FIG. 5. Amplitude-frequency curves for dynamic force $F_{sp}(V_1)$ in the nonlinear Model I for $K_{123} = -0.05$, $P_0 = 2.5$ with nonlinear functions (2.1) – (2.4).

The application ranges of the functions (2.1) and (2.2) are shown in Fig. 6. This is done for $K_{123} = -0.025, -0.05, -0.1, -0.15$ for the first resonant region. Suitable curves are marked by dashed and continuous lines. These curves determine the amplitudes of the external loading (5.12) below which numerical solutions behave as harmonic functions with the period equal to the period of the external loading. The smallest values for P_0 are acceptable in the neighbourhood of the resonance. From Fig. 6 it also follows that for the fixed K_{123}, the application ranges are slightly wider in the case of the sinusoidal function (2.2). It is connected with the fact that taking into account (2.1), (2.2), and (2.5),

the function F_{sp} has higher maximum values using the sinusoidal function than using the polynomial function.

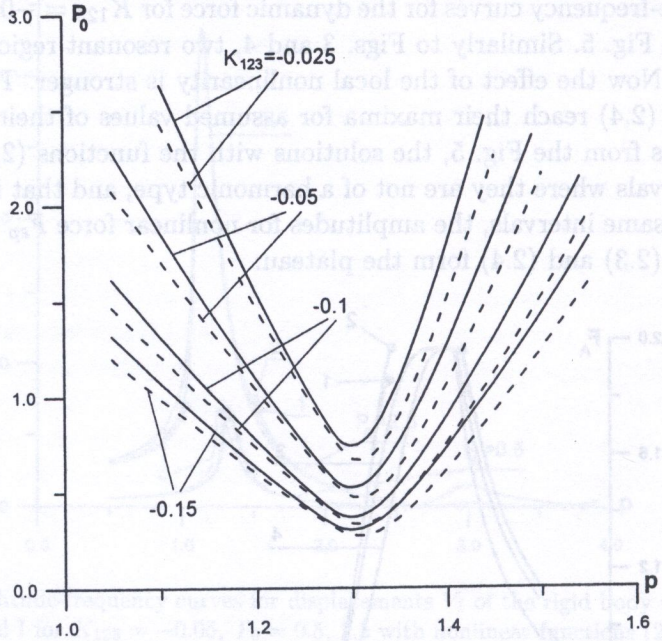

FIG. 6. Application ranges of the sinusoidal function (continuous lines) and polynomial function (dashed lines) for the Model I with $K_{123} = -0.025, -0.05, -0.1, -0.15$.

No restrictions similar to those connected with the application of the nonlinear functions (2.1) and (2.2) have been found in the case of functions (2.3) and (2.4). Thus, the nonlinear functions (2.3) and (2.4) can be used in the discussion of the influence of various parameters on the dynamic behaviour of the considered models.

6. SOLUTION OF THE NONLINEAR MODEL II.

The Model II differs from the Model I shown in Fig. 2 as far as the conditions in the joint $x = -l_1 \sin\alpha$, $y = 0$ ($x_1 = x_3 = 0$) are concerned. Now, the rigid body m_3 is neglected, and the ends of members (1) and (3) are fixed. In the linear case this model corresponds to the Model I in [3].

The determination of displacements of truss members in the nonlinear Model II is reduced to solving equations of motion (5.1) with initial conditions (5.2), with boundary conditions $(5.3)_3 - (5.3)_6$, and with two additional boundary conditions

$$u_1(x_1, t) = 0 \quad \text{for} \quad x_1 = 0,$$
$$u_3(x_3, t) = 0 \quad \text{for} \quad x_3 = 0. \tag{6.1}$$

In nondimensional quantities (5.5) the problem leads to solving equations (5.6) with (5.7), $(5.8)_3 - (5.8)_6$, and with (6.1) in the unchanged form because bars denoting nondimensional quantities are omitted for convenience.

Now, the solution of equations (5.6) are sought in the form

$$
\begin{aligned}
u_1(x_1,t) &= f_1(t - x_1 + l_1) + g_1(t + x_1 - l_1),\\
u_2(x_2,t) &= f_2(t - x_2 + l_2) + g_2(t + x_2 - l_2),\\
u_3(x_3,t) &= f_3(t - l_2 - x_3 + l_3) + g_3(t - l_2 + x_3 - l_3).
\end{aligned} \tag{6.2}
$$

Comparing the solution (5.9) for the nonlinear Model I with the solution (6.2) one can notice that these solutions differ only in arguments of the function f_3. Now, according to (3.5) $t_{f3} = t_{g3} = l_2$ and $x_{f3} = x_{g3} = l_3$.

Substituting (6.2) into the boundary conditions (6.1), $(5.8)_3 - (5.8)_6$, and denoting the largest argument in each equality by z, one obtains the following equations for unknown functions f_i, g_i, i=1,2,3:

$$
\begin{aligned}
&f_1(z) = -g_1(z - 2l_1),\\
&f_2(z) = -g_2(z - 2l_2) - [f_3(z - 2l_2) + g_3(z - 2l_2)]sin\beta,\\
&f_3(z) = -g_3(z - 2l_3),\\
&r_1 g_1''(z) = P(z) + r_2 g_1'(z) + r_3 f_1''(z) + r_4 f_1'(z) + r_5 f_2''(z) + r_6 f_2'(z)\\
&\qquad\qquad - F_{sp}\left(\frac{f_1(z) + g_1(z)}{\cos\alpha}\right),\\
&g_2(z) = -f_2(z) + [f_1(z) + g_1(z)]\cos\beta/\cos\alpha,\\
&r_7 g_3''(z) + r_8 g_3'(z) + r_9 g_3(z) = r_{10} f_3''(z) + r_{11} f_3'(z) + r_{12} f_3(z)\\
&\qquad\qquad + r_{13} g_2''(z) + r_{14} g_2'(z),
\end{aligned} \tag{6.3}
$$

where constants r_i, i=1,2,...,14, are defined by (5.11).

Exemplary numerical calculations using equations (6.3) are performed for parameters (5.14) with $R_3 = 0$. Though the method applied in the paper allows to determine displacements in arbitrary cross-sections of the members of the considered nonlinear Model II, for the sake of clarity in the numerical discussion the displacements V_1 of the rigid body m_1 in the steady state are determined. The external force is assumed in the form (5.12).

In Fig. 7 are plotted the amplitude-frequency curves for the displacement V_1 for $K_{123} = -0.05$ and $P_0 = 0.5$, 2.5 using four nonlinear functions (2.1) – (2.4). The diagrams include three resonant regions. The nonlinear effects are significant

in the first resonant region. For the amplitude P_0 of the external loading (5.12) equal to 0.5 the diagrams with functions (2.2) – (2.4) are similar. Only when using the polynomial function (2.1), similarly to the case of the Model I, there exists the interval of frequency p where the numerical solution diverges to infinity. The extreme values of p are marked by spots. For $P_0 = 2.5$ by spots are marked extreme values of p for the polynomial function as well as for the sinusoidal function. Within these intervals the solution does not behave as a harmonic function. Such limitations are not noted using the functions (2.3) and (2.4). Diagrams with the use of these functions practically coincide with each other.

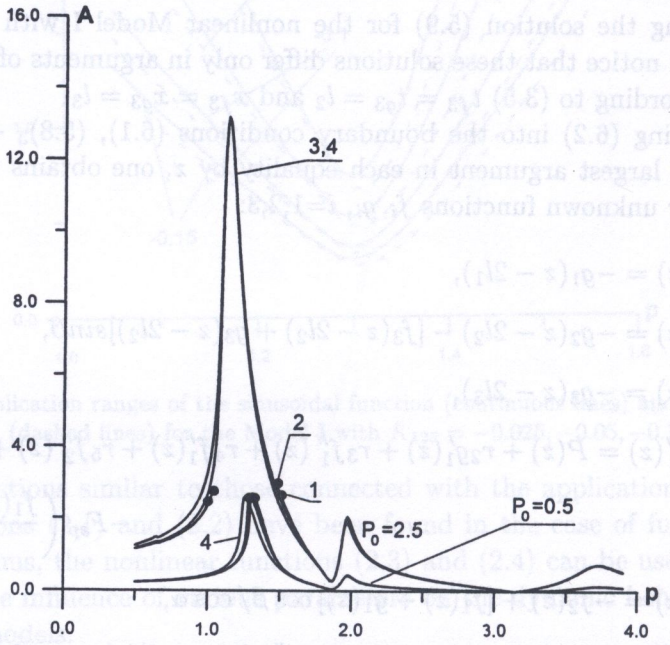

FIG. 7. Amplitude-frequency curves for displacements V_1 of the rigid body m_1 in the nonlinear Model II for $K_{123} = -0.05$, $P_0 = 0.5, 2.5$ with nonlinear functions (2.1) – (2.4).

Amplitude-frequency curves for the amplitude of the dynamic force F_{sp} for $K_{123} = -0.05$ and $P_0 = 0.5$ are plotted in Fig. 8. The maximal amplitudes are obtained for the sinusoidal function (2.2) and the smallest ones for the exponential function (2.4). Similarly to the displacements V_1, the spots determine the interval where the solution diverges to infinity when using the polynomial function (2.1).

Amplitude-frequency curves for the amplitude of the dynamic force F_{sp} for $K_{123} = -0.05$ and $P_0 = 2.5$ are plotted in Fig. 9. The diagrams include three resonant regions. In the first resonant region the spots determine intervals where the solution does not behave as a harmonic function. This concerns the functions

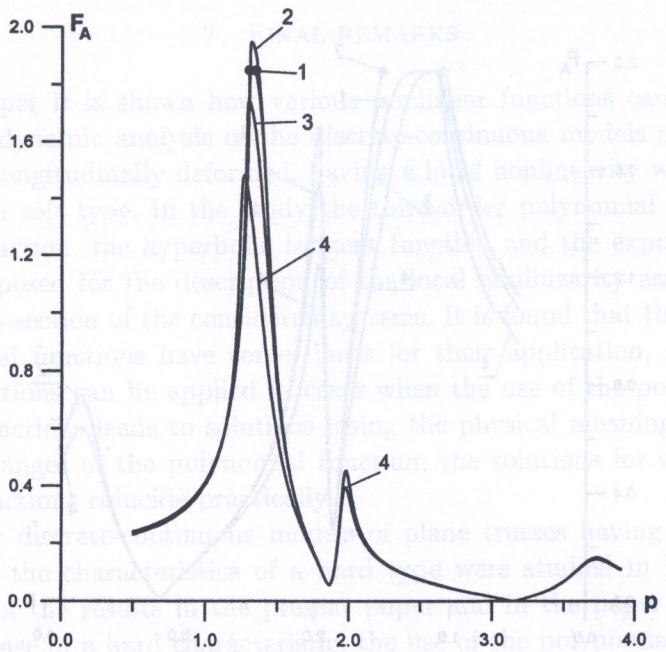

FIG. 8. Amplitude-frequency curves for dynamic force $F_{sp}(V_1)$ in the nonlinear Model II for $K_{123} = -0.05$, $P_0 = 0.5$ with nonlinear functions (2.1) – (2.4).

(2.1) and (2.2). The remaining functions in the first resonant region form the plateau. The plateau takes place in the cases when the dynamic force achieves its maximum value for assumed parameters occurring in the function (2.1). In the second resonant region the maximum amplitudes for the force are obtained using the functions (2.1) and (2.2) and the minimal ones for the function (2.4). Similar behaviour of the solution is noted in the third resonant region.

From Figs. 7 – 9 it follows that for the assumed parameters for the Model II some restrictions occur for the polynomial function (2.1) and the sinusoidal function (2.2). They are noted in the first resonant region. So, application ranges for these functions are shown in Fig. 10. They are done for $K_{123} = -0.025, -0.05, -0.1, -0.15$. Suitable curves are marked by dashed and continuous lines. These curves, similarly as in Fig. 6 for the Model I, determine the amplitudes P_0 of the external loading (5.12) below which numerical solutions behave as harmonic solutions with the periods equal to the periods of the external loading. The smallest amplitudes are acceptable in the neighbourhood of the resonance.

Comparing the appropriate diagrams in Figs 3 – 6 for the Model I with those in Figs 7 – 10 we can see that the application ranges of the functions describing the local nonlinearity in both the models are practically the same, however we can notice significant differences in amplitude-frequency diagrams for the displacement V_1 and for the force F_{sp}.

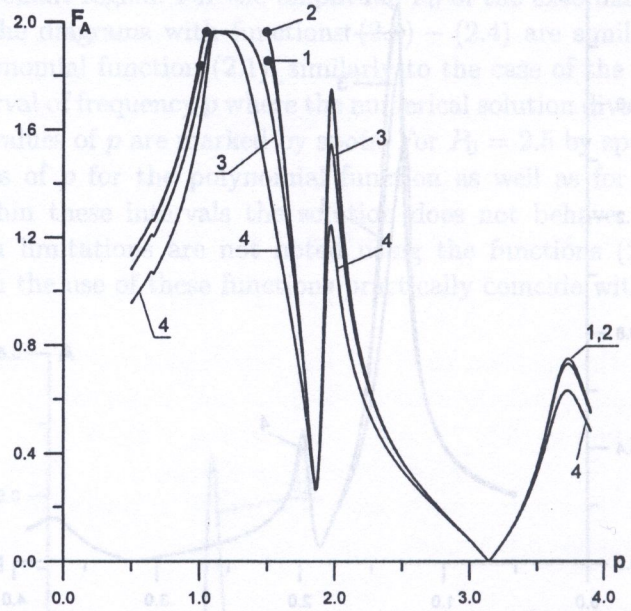

FIG. 9. Amplitude-frequency curves for dynamic force $F_{sp}(V_1)$ in the nonlinear Model II for $K_{123} = -0.05$, $P_0 = 2.5$ with nonlinear functions (2.1) – (2.4).

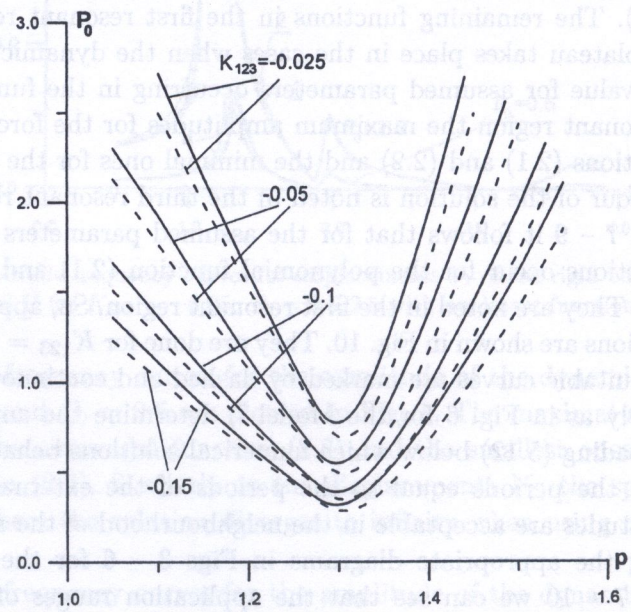

FIG. 10. Application ranges of the sinusoidal function (continuous lines) and polynomial function (dashed lines) for the Model II with $K_{123} = -0.025, -0.05, -0.1, -0.15$.

7. Final remarks

In the paper it is shown how various nonlinear functions can be incorporated in the dynamic analysis of the discrete-continuous models of multi-mass rod systems longitudinally deformed, having a local nonlinearity with the characteristic of a soft type. In the study the third-order polynomial function, the sinusoidal function, the hyperbolic tangent function and the exponential function, are proposed for the description of the local nonlinearity assumed in the selected cross-section of the considered systems. It is found that the polynomial and sinusoidal functions have some limits for their application, and that the last two functions can be applied in cases when the use of the polynomial and sinusoidal functions leads to solutions losing the physical meaning. Within the application ranges of the polynomial function, the solutions for all considered nonlinear functions coincide practically.

Nonlinear discrete-continuous models of plane trusses having local nonlinearities with the characteristics of a hard type were studied in [1]. From the comparison of the results in the present paper and in the paper [1] it follows that in the case of a hard characteristic, the use of the polynomial function for its description gives satisfactory results, while in the case of a soft characteristic one may expect certain inconveniences. Moreover, the jumps of the amplitudes of displacements and forces are observed in models having local nonlinearities with the characteristics of a hard type.

References

1. A. Pielorz, *Nonlinear discrete-continuous models in dynamic investigations of plane truss members*, Engineering Transactions, **45**, 133–152, 1997.

2. J.M. Gere, W. Weaver, *Analysis of framed structures*, D.Van Nostrand Company, Inc. New York 1965.

3. W. Nadolski, A. Pielorz, *The use of elastic waves in dynamic investigations of plane truss members*, The Archive of Mechanical Engineering, **43**, 105–123, 1996.

4. A. Niemierko, *On the trusses* [in Polish], WKiŁ, Warsaw 1987.

5. Chr. Boiler, T. Seeger, *Materials data for cyclic loading, Parts A-E*, Elsevier, New York 1987.

6. H.B. Stewart, J.M.T. Thompson, Y. Ueda, A.N. Lansbury, *Optimal escape from potential wells – patterns of regular and chaotic bifurcation*, Physica D, **85**, 259–295, 1995.

7. W. Gutkowski, J. Bauer, Z. Iwanow, *Explicit formulation of Kuhn-Tucker necessary conditions in structural optimization*, Computers and Structures, **37**, 753–758, 1990.

8. U. Bernhard, W. Hauger, *The propagation of waves in impact-loaded spatial trusses*, Archive of Applied Mechanics, **63**, 556–566, 1993.

9. T.P. DESMOND, *Theoretical and experimental investigation of stress waves in junction of three bars*, J. Applied Mechanics, **48**, 148–154, 1981.

10. J.P. LEE, *Elastic waves produced by longitudinal impact on system with symmetrically branched rods*, Int. J. Solids Structures, **8**, 699–707, 1972.

11. P. HAGEDORN, *Non-linear oscillations*, Clarendon Press, Oxford 1981.

12. A. PIELORZ, *Non-linear vibrations of a discrete-continuous torsional system with non-linearities having characteristic of a soft type*, J. Sound and Vibration, **225**(2), 375–389, 1999.

Received December 19, 2000.